ICEBERG SIZE AND ORIENTATION ESTIMATION USING SEAWINDS

Keith M. Stuart and David G. Long

Brigham Young University, MERS Laboratory, 459 CB, Provo, UT 84602

1. INTRODUCTION

The SeaWinds scatterometer was originally designed to measure surface winds over the ocean. In addition to SeaWinds' primary goals, high-resolution data products specifically enable valuable contributions in the Antarctic. Even though SeaWinds was never designed to track icebergs, an extensive Antarctic iceberg database detailing positions of large tabular icebergs has been derived from the data and is used in this study. From high-resolution backscatter images, iceberg location and backscatter values are cataloged on a daily basis [1].

Here, we extend the analysis of SeaWinds iceberg observations to include size and orientation via maximum-likelihood (ML) estimation techniques. First, the background for large tabular iceberg observation by SeaWinds backscatter measurements is reviewed. Next, an elliptical model is chosen to characterize large tabular icebergs. An objective functions relating measured backscatter given model-based backscatter is developed, based on the ML estimation approach. Next, the utility of the estimate is analyzed in simulation and a case study of iceberg A22a is presented. Finally, subsequent size and orientation estimates are compared with reports collected by the United States National Ice Center (NIC).

2. BACKGROUND

SeaWinds is a Ku-band scanning pencil-beam scatterometer aboard the QuikSCAT spacecraft and is designed to determine the normalized radar cross section, σ°, of the Earth's surface. Its sun-synchronous orbit allows for complete daily coverage of the polar regions, making it an ideal platform for high-latitude studies. SeaWinds has two scanning conical beams. The outer beam is vertically polarized at a nominal incidence angle of 54°; the inner beam is horizontally polarized at a nominal incidence of 46°. This design provides for four independent looks of the region lying within the inner swath and two independent looks of targets contained within the outer swath [2, 3].

Using onboard range-Doppler processors, SeaWinds backscatter values for each microwave pulse are separated into regions called slices where each has a separate σ° value. Because of the rapid roll-off of the aperture response function corresponding to each slice, individual response patterns are frequently represented as a binary mask corresponding to the 6 dB contour of each slice footprint, measuring approximately 6 x 25 km.

Because each range-Doppler-filtered slice has a large spatial footprint compared to the operating wavelength, each σ° measurement may be modeled as a linear combination of spatial backscatter distributions where

$$\sigma^\circ = \frac{\int A(\tau)\sigma^\circ_{pt}(\tau)d\tau}{\int A(\tau)d\tau} + \nu \tag{1}$$

where σ° is a SeaWinds backscatter measurement, A is the antenna gain of the 2-dimensional ground illumination footprint, $\sigma^\circ(\tau)$ is the spatial distribution of σ° at the surface, and ν is the cumulative noise term.

By utilizing backscatter differences in backscatter between glacial ice, sea ice, and sea water, it is possible to detect and track large Antarctic icebergs. These floating glacial ice fragments must generally be larger than 5 km to be detected and are typically characterized as a rough ice plateau above the water. Using reconstruction-enhanced scatterometer images, these icebergs are tracked on a daily basis and are cataloged as part of the Scatterometer Record Pathfinder Project at Brigham Young University's Microwave Earth Remote Sensing (MERS) Laboratory [1]. To supplement daily iceberg position reports, this paper presents an automated approach to estimate the size and orientation of large tabular icebergs using a ML estimation approach.

3. THEORY

Rather than use images, the proposed approach uses individual slice measurements and their binary spatial response functions. Backscatter values are collected around an iceberg such that the iceberg and the immediately-surrounding background sea water or sea ice is observable. Given this assumption, Eq. 1 simplifies to

$$\sigma^\circ = c\sigma^\circ_{berg} + (1-c)\sigma^\circ_{back} + \nu. \tag{2}$$

where σ°_{berg} and σ°_{back} represent the average backscatter values of the iceberg and the surrounding medium (sea water or sea ice), c is the ratio of the ground spatial footprint over glacial ice to the background area and ν is the cumulative noise term.

The cumulative distribution of each σ° measurement is normally distributed according to

$$f(\sigma^\circ) = \frac{1}{\sqrt{2\pi}\eta} exp\left\{-\frac{(\sigma^\circ)^2}{2\eta^2}\right\} \tag{3}$$

where η is the variance of σ° [3].

A simple model is chosen to describe the area and approximate shape of a large tabular iceberg. This model is a super-ellipse of form

$$\left|\frac{x-x_c}{a}\right|^n + \left|\frac{y-y_c}{b}\right|^n = 1 \tag{4}$$

where x_c and y_c are the center parameters, a and b are the major and minor axis lengths and n is the super-ellipse parameters where $n > 0$. While irregularly shaped icebergs are not elliptical, this model is effective in generalizing iceberg shape for purposes of parameter estimation. The model parameters consist of those defined in Eq. 2 and 4, specifically σ°_{berg}, σ°_{back}, c, x_c, y_c, a, b, n, and an angle parameter for model orientation. These parameters constitute the vector $\bar{p}$, the model parameter vector to estimate.

The estimation process is characterized by minimizing the radar backscatter measured by SeaWinds given backscatter calculated via the model. This objective function is

$$f(\sigma^\circ|\sigma^\circ_s(\bar{p})) = \frac{1}{\sqrt{2\pi}\eta_s} exp\left\{-\frac{[\sigma^\circ - \sigma^\circ_s(\bar{p})]^2}{2\eta_s^2}\right\} \tag{5}$$

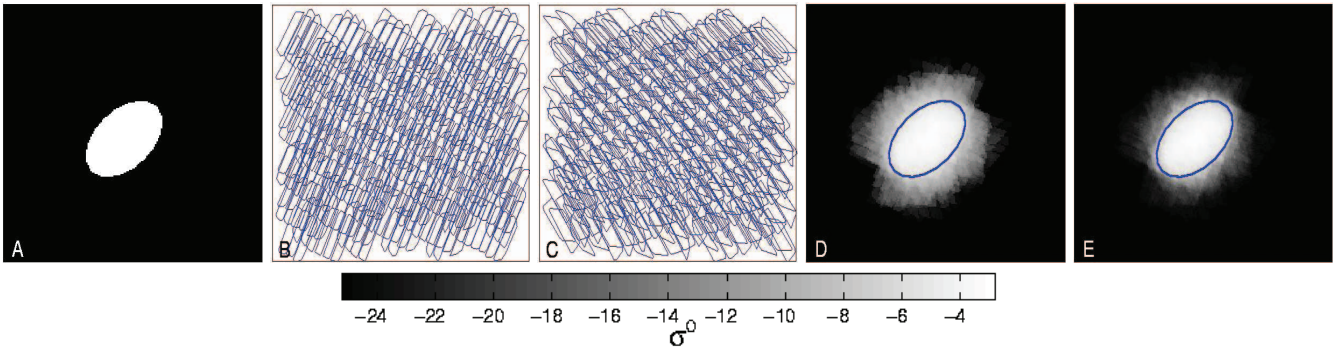

Fig. 1. Simulation of estimating the size and orientation of an elliptical iceberg. A) The initial binary iceberg model. B) 6 dB-contour plot of the forward-looking SeaWinds slice measurements for a single pass. There are approximately 330 slices, each approximately 25 x 6km in dimension. C) Corresponding aft-looking slice measurements for the same pass. D) Geometric-average backscatter composite in dB. E) Geometric-average composite in linear space. Estimated parameters conformed exactly to the initial model and are juxtaposed over each composite image. Images correspond to approximately 300 x 300 km.

where σ° is the backscatter value measured by SeaWinds and σ_s° is the model-based backscatter based upon $\bar{p}$ from Eq. 4. From Eq. 5, the ML objective function may be expressed as

$$\bar{p}^* = \underset{\bar{p}}{argmax} \left\{ \sum_j \left[-\frac{[\sigma^\circ - \sigma_s^\circ(\bar{p})]^2}{2\eta_s^2} - log(\sqrt{2\pi}\eta_s) \right] \right\} \tag{6}$$

where the objective function is summed over j, the count of σ° measurements in the frame of estimation, and with optimal model parameters being denoted $\bar{p}^*$.

For the noise-free case, Eq. 6 has a single maxima which is found by searching $\bar{p}$. Figure 1a illustrates a simulated iceberg. The 6 dB-contour of the forward and aft-looking slice aperture responses over the iceberg for a single pass are displayed in Fig. 1b,c. Composite backscatter images are displayed in Fig. 1d,e for the linear and geometric average cases in both dB and linear space. As expected, estimated parameters converge to the initial model parameters. Notice that the composite backscatter image that most resembles the original model is the geometric average, displayed in linear space.

4. CASE STUDY

The technique is applied to SeaWinds backscatter measurements of iceberg A22a. In a noisy environment, Eq. 5 is not guaranteed is have a single solution; therefore, an exhaustive search of $\bar{p}$ is conducted. Iceberg A22a is selected because it is non-circular, is tracked for an extended period of time away from sea ice, and because collocated high-resolution imagery is available.

Two days are highlighted in this study: 2006JD110 and 2006JD303. For these days, annotated high-resolution images of iceberg A22a are available from DMSP and MODIS and are displayed in Fig. 2a,c. Corresponding SeaWinds backscatter measurements for these days and are displayed in Fig. 2b,d. Models based on iceberg size and orientation estimates are also juxtaposed on the backscatter images. NIC reports and SeaWinds estimates are

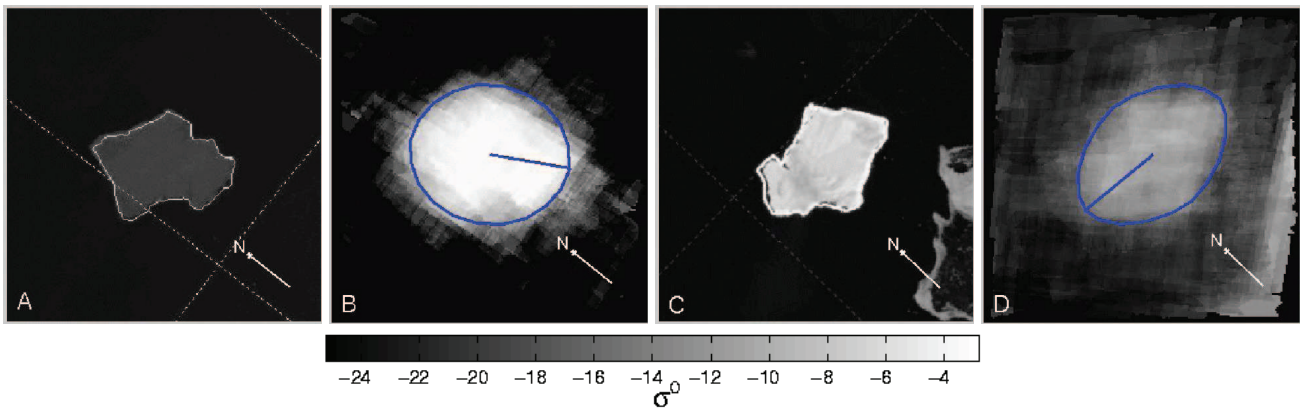

Fig. 2. Images of iceberg A22a on a) 2006JD110 from DMSP IR and c) 2006JD303 from MODIS. Corresponding horizontally-polarized SeaWinds backscatter images are in (b,d). Models based on iceberg size and orientation estimates are juxtaposed on the backscatter images. On JD303, iceberg σ° is lower due to surface melt conditions. Also, ocean σ° is higher due to increased surface roughness caused by local wind conditions. For iceberg size comparisons, see Table 1.

Table 1. Major and minor axis comparisons of iceberg A22a between NIC reports and SeaWinds estimates on 2006 Julian Days 110 and 303.

	2006JD110		2006JD303	
	Major Axis	Minor Axis	Major Axis	Minor Axis
NIC Report	68 km	51 km	68 km	51 km
SeaWinds ML Estimate	66 km	57 km	70 km	49 km
Percent Error	3%	12%	3%	4%

compared in Table 1. Note the consistency of iceberg orientation in the high-resolution images and the ML estimates. ML estimates coincide with iceberg dimensions reported by the NIC via high-resolution imagery to within an average of 94%.

5. REFERENCES

[1] Microwave Earth Remote Sensing Laboratory, "Scatterometer Climate Record Pathfinder," http://www.scp.byu.edu/, update 2009.

[2] D.S. Early and D.G. Long, "Image Reconstruction and Enhanced Resolution Imaging from Irregular Samples," *IEEE Transactions on Geoscience and Remote Sensing*, vol. 39, no. 2, pp. 291–302, 2001.

[3] M.W. Spencer and D.G. Long, "Improved Resolution Backscatter Measurements with the SeaWinds Pencil-Beam Scatterometer," *IEEE Transactions on Geoscience and Remote Sensing*, vol. 38, no. 1, pp. 89–104, 2000.